DOI: 10.24874/ti.2006.08.25.03

Tribology in Industry

www.tribology.rs

RESEARCH

Multi-Response Optimization of CNC Milling Parameters for SUS316 Diffuser Guide Vanes: Effects on Surface Roughness, Machining Time, and Tool Wear

Muhamad Daffa Aditya Eka Pratama[a], Benidiktus Tulung Prayoga[a,*], Galuh Bahari[a], Handoko[a]

[a]*Department of Mechanical Engineering, Vocational School, Universitas Gadjah Mada, Yogyakarta, 55281, Indonesia.*

Keywords:

Machining parameters
SUS316
Surface roughness
Machining time
Tool wear

* Corresponding author:

Benidiktus Tulung Prayoga
E-mail: beni@ugm.ac.id

Received: 24 October 2025
Revised: 29 November 2025
Accepted: 13 March 2026

A B S T R A C T

Stainless Steel 316 (SUS316) is widely employed in critical industrial components due to its mechanical strength and corrosion resistance, but its low thermal conductivity and high ductility make it a difficult to machine material. This study investigates the influence of spindle speed, feed rate, and depth of cut on surface roughness (Ra), machining time, and tool wear (V_B) in CNC milling of SUS316 Diffuser Guide Vanes. A Response Surface Methodology (RSM) with Box–Behnken Design (BBD) was applied, followed by Analysis of Variance (ANOVA) and multi-response optimization using a desirability function. Results reveal that Ra is mainly controlled by spindle speed and feed rate, machining time is governed by feed rate and depth of cut, while V_B exhibits a non-linear dependence on feed rate. The integrated optimization identified a parameter setting that simultaneously minimizes Ra, machining time, and V_B with a high desirability index, providing a validated guideline for balancing machining quality, productivity, and tool life. The optimal values of the input parameters determined to be a spindle speed of 700 RPM, a feed rate of 70 mm/min, and a depth of cut of 1 mm. The best results obtained are surface roughness of 0.185 µm, a machining time of 1737 s, and a flank wear width (V_B) of 51.67 µm, with a high composite desirability value of 0.832.

1. INTRODUCTION

The increasing demand for high-performance industrial components in aerospace, chemical, and biomedical sectors has driven the widespread adoption of advanced engineering materials with superior mechanical and chemical properties. Among these, austenitic Stainless Steel 316 (SUS316) is one of the most widely applied alloys due to its excellent mechanical strength, toughness, and resistance to chloride-induced corrosion and pitting [1,2]. Its enhanced

corrosion resistance, attributed to higher nickel and molybdenum content compared to Stainless Steel 304, makes it indispensable in aggressive environments such as marine structures, chemical plants, and biomedical implants [3]. However, despite these advantages, SUS316 is universally recognized as a "difficult-to-cut" material [4]. Its low thermal conductivity impedes efficient heat dissipation during machining, while its high ductility promotes built-up edge (BUE) formation, rapid tool wear, and poor surface integrity [5,6].

Achieving high-quality components from challenging materials like SUS316 necessitates a careful balance of multiple, often conflicting, performance metrics. Surface roughness (R_a), a measure of fine-scale deviations on a workpiece surface, is a critical indicator of product quality and performance [7]. These irregularities are directly influenced by machining parameters, cutting tool geometry, and phenomena like chip flow damage [8,9]. Concurrently, tool wear, defined as the gradual degradation of the cutting edge, directly impacts dimensional accuracy and surface integrity [10,11]. Flank wear (V_B), being the most common and easily measured type, is a widely accepted metric for determining tool life, with ISO 8688-2 defining its operational limits [12,13]. Finally, machining time, the duration required for a cutting pass, serves as a key indicator of productivity [14]. These three responses surface roughness, tool wear, and machining time are highly interdependent and sensitive to the selected machining parameters. An improper parameter set can accelerate tool wear, which in turn degrades surface quality, compromises dimensional accuracy, and increases total machining time due to frequent tool replacements [15] Therefore, optimizing these parameters is not merely beneficial but essential for achieving a process that is efficient, cost-effective, and capable of producing high-quality components consistently.

To address these machining challenges, numerous studies have explored the optimization of parameters for stainless steels. Methodologies like the Taguchi method have been instrumental in identifying key influential factors. For instance, Equbal et al. [3] investigated the CNC milling of AISI 316 and concluded that feed rate and depth of cut were the most influential parameter affecting surface roughness. Similarly, Shelar et al. [16] using a Taguchi L27 design for SUS316, identified feed rate as the most significant factor influencing both surface roughness (R_a) and Material Removal Rate (MRR). Expanding the scope, Shinde and Jadhav [17] optimized for multiple responses on 316L steel and incorporated Grey Relational Analysis (GRA) for multi-objective optimization.

More recently, Response Surface Methodology (RSM) paired with a Box-Behnken Design (BBD) has become a prevalent technique for its efficiency in modeling complex, non-linear relationships. BBD is particularly suitable for optimizing processes, as it can effectively model both linear and quadratic effects with a minimal number of experimental runs [18,19]. Its successful application has been demonstrated across various materials and objectives. For instance, Hernández-González et al. [20] applied an RSM-BBD approach to the milling of Stainless Steel 304, where they identified separate optimal settings for the conflicting goals of maximizing MRR and minimizing surface roughness. The methodology is also proven effective in more complex scenarios involving nano-lubricants; Peña-Parás et al. [21,22] successfully used an RSM-BBD approach to establish a single set of optimal parameters for multi-response goals including tool wear, energy consumption, and surface roughness during the milling of both AISI 1018 and AISI 4340 steels with MMT and HNT nano-additives, respectively. Further demonstrating the method's utility on challenging materials. Policena et al. [23] used a BBD to optimize the dry finishing end-milling of duplex stainless steel UNS S32205, determining that feed per tooth (f_z) was the most significant factor for achieving a validated low surface roughness of R_a = 0.182 µm. Nevertheless, despite extensive research on stainless steel machining, a comprehensive multi-response optimization framework that simultaneously addresses surface quality, productivity, and tool longevity in SUS316 milling remains limited.

This study aims to address the identified gap by performing a multi-response optimization for the CNC milling of SUS316. The novelty of this work lies in its integrated approach using Response Surface Methodology (RSM) with a Box-Behnken Design (BBD), coupled with a desirability function, to find a single, balanced set of optimal

parameters that concurrently considers surface roughness (R_a), machining time, and tool wear (V_B). The primary contribution of this research is the provision of a verified optimal setting that resolves the trade-offs between surface roughness, machining time, and tool life, offering a practical and robust solution for industrial applications. To the best of our knowledge, this is the first integrated study applying RSM-BBD desirability function for simultaneous optimization of R_a, machining time, and V_B in SUS316 milling

2. EXPERIMENTAL DETAILS

2.1 Material and equipment

The shop drawing for the diffuser guide vanes is presented in Fig. 1. The workpiece material used in this study was stainless steel 316 (SUS316). All specimens were initially pre-machined on a conventional lathe, as shown in Fig. 2(a). The workpiece geometry consisted of two main sections. The upper section comprised a circular contour with a diameter of 50 mm and a thickness of 7.5 mm, which constituted the primary milling surface. The lower section was a cylindrical shank with a diameter of 24 mm and a length of 21.5 mm, designed specifically for clamping purposes. During CNC milling, this lower section was securely held in the chuck, as illustrated in (Fig. 2b).

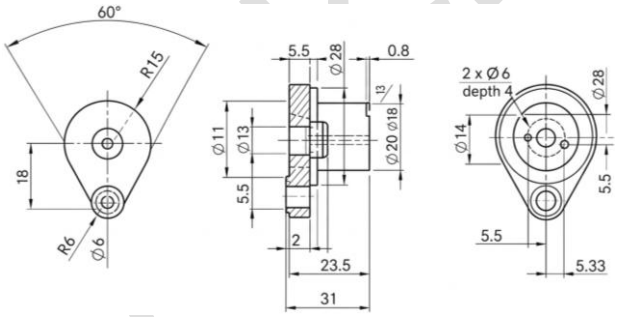

Fig. 1. Shop drawing of Diffuser guide vanes.

The experiments were conducted on a 5-axis CNC Vertical Machining Center (DMG Mori DMF 180 linear) with output power of 38.8 kW. A standard tool holder with a diameter of 25 mm, supplied as an original accessory for the DMF 180 Linear, was employed. The cutting tool consisted of three PVD AlTiCrN-coated carbide inserts. To eliminate the influence of prior tool degradation and ensure the reliability of wear measurements, a new set of cutting inserts was used for each experimental run.

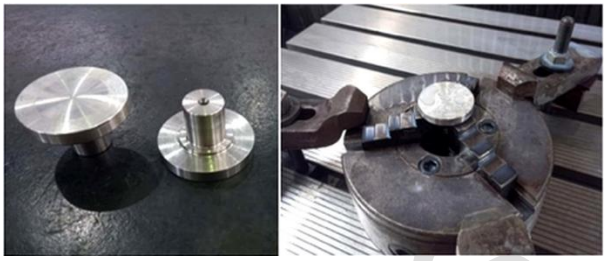

(a) (b)

Fig. 2. The milling workpieces (a) pre-machined workpiece has undergone initial turning (b) Clamping of pre-machined workpiece.

The cutting speed was varied at three levels: 39.25 m/min, 47.10 m/min, and 54.95 m/min. Depth of cut (ap) and feed rate were selected as the primary independent variables and were varied according to the experimental design. The specific levels of these parameters are summarized in Table 1. All experiments were performed under wet milling conditions with a constant supply of coolant.

2.2 Experimental design

The experimental design and subsequent statistical analysis were carried out using statistical software. Following the approach introduced in the Introduction, a Box–Behnken Design (BBD) under the Response Surface Methodology (RSM) framework was employed to generate the experimental matrix.

The design comprised 15 randomized experimental runs, enabling efficient estimation of linear, quadratic, and interaction effects with a reduced number of experiments compared to a full factorial design. The BBD excludes extreme corner points of the cubic design space, which minimizes the risk of conducting experiments at potentially unsafe parameter combinations while maintaining high predictive capability for response modelling.

The scope of the optimization was limited exclusively to the top-side contouring operation of the diffuser guide vanes. Drilling and pocketing processes were not included in the analysis. The top-side contouring process and corresponding tool paths are illustrated in Fig. 3.

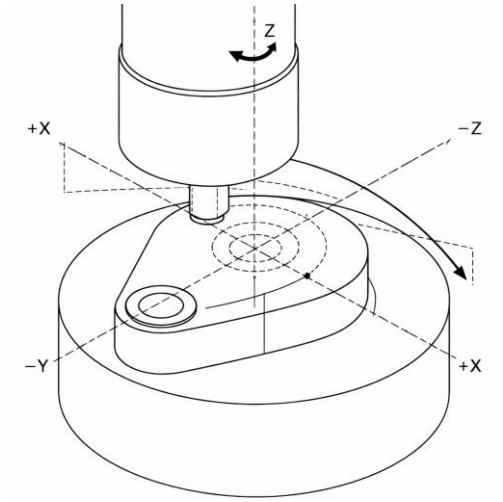

Fig. 3. CAD/CAM simulation of the Diffuser Guide Vanes machining stages, showing the main contour and upper surface operations with their corresponding tool paths.

2.3 Response measurement

Three output responses were measured after each experiment. The first output response was surface roughness (R_a). This value was obtained for each specimen by averaging measurements from four predetermined points on the top machined surface as shown in Fig. 4. These measurements were performed using a TIME 3200 Surface Roughness Tester (TR200).

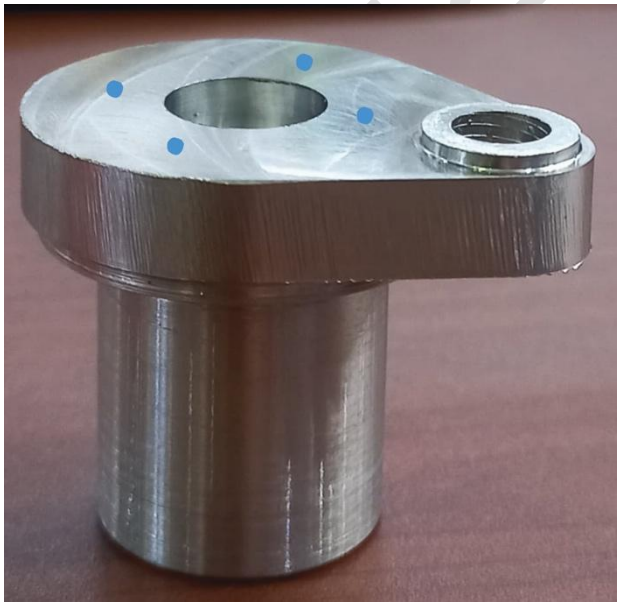

Fig. 4. Finished part, the dots are locations of surface roughness measurements.

The second response was machining time, defined as the active cutting duration encompassing all tool movements from the start to the end of the program. This time was recorded directly from the machine's integrated counter. Theoretically, the machining time for a single pass (T_m) is determined by the total feed length (L_t) and the feed rate (V_f), as expressed in Equation (1). The feed rate (V_f) is, in turn, a function of the spindle speed (n), feed per tooth (f_z), and the number of inserts (Z), as calculated in Equation (2). Consequently, the total machining time (T_{Total}) needed to complete an entire workpiece is determined by multiplying the time per pass by the total number of cutting passes, as shown in Equation (3).

$$T_m = \frac{L_t}{V_f} \tag{1}$$

$$V_f = n \times f_z \times Z \tag{2}$$

$$T_{total} = \frac{L_t}{V_f} \times \frac{Total\ Depth}{a_p} \tag{3}$$

The third and final output response was tool wear. In this study, the flank wear assessment included two components: the wear length along the main cutting edge and the flank wear width (V_B). Both values, measured in microns (μm), were recorded for all three inserts tool after each test using an Olympus Stereo Microscope SZ-PT. An insert was considered to have reached its wear limit if the average flank wear width (V_B) reached 0.3 mm, in accordance with the ISO 8688-2 standard. Although the machining time can be theoretically determined using Equation (3), it was also treated as an experimental response variable in this study. The actual machining time is affected by several non-ideal factors, including toolpath complexity, machine acceleration and deceleration, and tool approach or retract movements. Furthermore, machining time was considered as a response variable because it represents one of the key objectives in the multi-response optimization, together with surface roughness and tool wear.

2.4 Data analysis

The experimental data were initially validated through normality, homogeneity, and outlier tests, as summarized in Table 2. Subsequently, Analysis of Variance (ANOVA) was conducted to assess the significance of linear, quadratic, and interaction effects of the machining parameters on each response.

Finally, multi-response optimization was performed using a desirability function approach. The optimization objective was set to "smaller is better" for all three responses surface roughness, machining time, and tool wear to identify a single, balanced set of optimal machining parameters.

Table 1. Input parameters for the design of experiments.

Run	Spindle Speed (rpm)	Feed Rate (mm/min)	Depth of Cut (mm)
1	500	70	0.75
2	700	70	0.75
3	500	90	0.75
4	700	90	0.75
5	500	80	0.5
6	700	80	0.5
7	500	80	1
8	700	80	1
9	600	70	0.5
10	600	90	0.5
11	600	70	1
12	600	90	1
13	600	80	0.75
14	600	80	0.75
15	600	80	0.75

Table 2. Results p-value for data validation tests.

Response	Normality Test	Homogeneity Test	Outlier Test	Lack-of-Fit Test
Ra	0.051	0.095	0.216	0.143
Machining Time (s)	>0.100	-	0.587	0.019
Wear Length (μm)	>0.100	0.518	0.437	0.424
V_B	>0.100	0.449	0.064	0.271

3. RESULT AND DISCUSSION

Prior to the main analysis, a series of statistical tests were conducted to validate the dataset for each response variable. The normality of data was assessed using the Ryan-Joiner test, homogeneity of variances was evaluated with the robust Levene's Test, and outliers were identified using Grubbs' Test. The results from Table 2. confirmed that the data for surface roughness (R_a) and tool wear (both wear length and flank wear width (V_B) successfully met all required assumptions. These responses passed the normality test (p-value > 0.05), homogeneity of variances test (p-value > 0.05), and showed no significant outliers or lack of fit (p-value > 0.05). This established the robustness and validity of the regression models developed for these two critical tribological responses. Conversely, the model for machining time exhibited a significant lack of fit (p-value = 0.019). The investigation revealed that this was not due to experimental error but rather a fundamental conflict between the deterministic, inverse mathematical relationship governing machining time and the empirical polynomial model used by the RSM.

Table 3. Average results of the output variables for each of the 15 combinations.

Run	R_a (mm)	Machining Time (s)	Wear Length (μm)	V_B
1	0.378	2492	633.334	55
2	0.245	2493	788	55.667
3	0.383	1949	750.334	54
4	0.441	1950	819.667	62
5	0.288	2983	702	61.334
6	0.252	2984	680.667	62.334
7	0.351	1523	1067	64.667
8	0.264	1523	968	64
9	0.234	3399	557.334	57.334
10	0.261	2660	502.334	44.334
11	0.191	1736	861.334	56.667
12	0.290	1358	905	60
13	0.242	2189	705.667	64.667
14	0.263	2186	627.667	69.334
15	0.252	2188	579	66

Table 3 shows the experimental results for surface roughness, machining time, wear length, and V_B. The shortest machining time was obtained at higher feed rates and greater depths of cut, which is consistent with the theoretical prediction given by Equation (3). As the machine, conditions, and toolpaths were identical for all experiments, the observed variation in machining time directly

stems from the changes in cutting parameters, aligning with the theoretical feed-rate relationship. The experimental validation was conducted to confirm that this theoretical trend remains valid under actual machining conditions.

Table 4. ANOVA of surface roughness.

Source	DF	Sum of Squares	Mean Squares	F	P-Value
Model	9	0.063116	0.007013	15.49	0.004
Linear	3	0.018756	0.006252	13.81	0.007
S	1	0.004901	0.004901	10.83	0.022
F	1	0.013387	0.013387	29.57	0.003
D	1	0.000469	0.000469	1.04	0.355
Square	3	0.033223	0.011074	24.47	0.002
S^2	1	0.021998	0.021998	48.60	0.001
F^2	1	0.003870	0.003870	8.55	0.033
D^2	1	0.005982	0.005982	13.22	0.015
2-WI	3	0.011137	0.003712	8.20	0.022
S*F	1	0.009240	0.009240	20.41	0.006
S*D	1	0.000619	0.000619	1.37	0.295
F*D	1	0.001278	0.001278	2.82	0.154
LoF	3	0.002043	0.000681	6.18	0.143
Pure Error	2	0.000221	0.000110	-	-
Total	14	0.065379	-	-	-

The ANOVA for surface roughness presented in Table 4. In these equations S, F, D, WI, and LoF represent the spindle speed, feed rate, depth of cut, way interaction, and lack of fit. Table 4 revealed that the regression model was statistically significant (p=0.004, F-value=15.49). The analysis identified that the linear terms of feed rate (p=0.003) and spindle speed (p=0.022) were the most significant factors affecting surface roughness. In contrast, the linear effect of depth of cut was not significant (p=0.355). The discussion of these results aligns with established machining principles. This is consistent with established machining principles: increasing feed rate enlarges the distance between tool marks, thereby worsening R_a, while higher spindle speed suppresses built-up edge (BUE) formation and produces a finer finish [14,15,22]. Furthermore, the significance of all quadratic terms and the two-way interaction between spindle speed and feed rate (p<0.05) indicates a complex, non-linear relationship. As visualized in the surface plots (Fig. 5), the lowest surface roughness is achieved at a combination of low feed rate and high spindle speed.

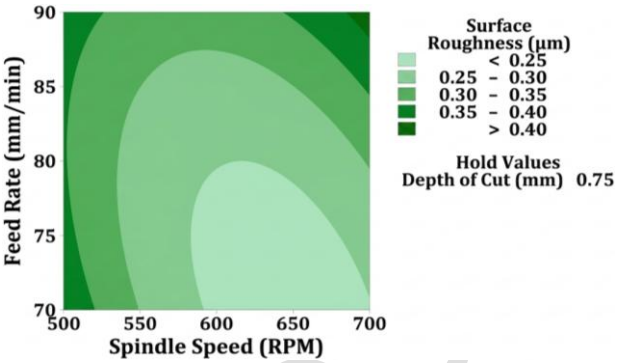

Fig. 5. Interaction between feed rate and spindle speed for surface roughness.

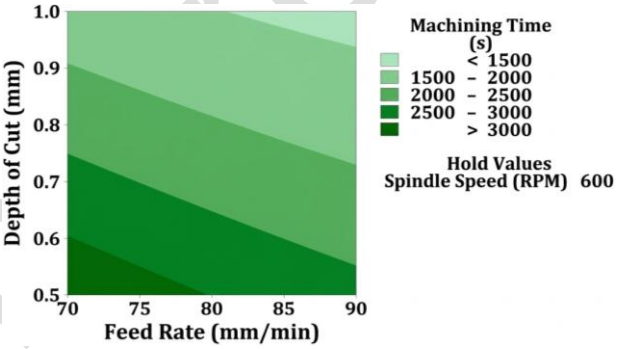

Fig. 6. Interaction between feed rate and depth of cut for machining time.

For machining time, the ANOVA results (Table 5) showed that feed rate (p=0.000) and depth of cut (p=0.000) were highly significant factors, while spindle speed had no significant effect (p=0.906). The dominance of depth of cut is attributed to its direct role in determining the total number of cutting passes required to achieve the final geometry (as describe in Equation (3)). Similarly, feed rate's significance stems from its function as the primary divisor in calculating the time per pass (see Equation (1)). This relationship is visualized in the contour plot (Fig. 6), which shows that the machining time decreases as both the feed rate and depth of cut increase. The best response for the fastest machining time occurs when these parameters are at their maximum levels, specifically a feed rate of 90 mm/min and a depth of cut of 1 mm. The lack of influence from spindle speed is explained by the experimental setup; the feed rate (mm/min) was programmed directly and not calculated as a function of spindle speed (as shown in Equation (2)), making it an independent variable in this context.

Table 5. ANOVA of machining time.

Source	DF	Sum of Squares	Mean Squares	F	P-Value
Model	9	4989521	554391	7.554,73	0,000
Linear	3	4937277	1645759	22.426,88	0,000
S	1	1	1	0,02	0,906
F	1	606651	606651	8.266,88	0,000
D	1	4330624	4330624	59.013,73	0.000
Square	3	19664	6555	89.32	0.000
S^2	1	3	3	0.03	0.859
F^2	1	4310	4310	58.74	0.001
D^2	1	16287	16287	221.95	0.000
2-WI	3	32581	10860	147.99	0.000
S*F	1	0	0	0.00	1.000
S*D	1	0	0	0.00	0.956
F*D	1	32580	32580	443.97	0.000
LoF	3	362	121	51.75	0.019
Pure Error	2	5	2	-	-
Total	14	4989888	-	-	-

It is important to note that the statistical model for machining time showed a significant Lack-of-Fit (p=0.019). This outcome was anticipated, as the relationship governing machining time is fundamentally deterministic and follows an inverse mathematical formula (Equations (1) and (3)), which is not perfectly represented by the polynomial model of RSM. However, despite this limitation in the model's predictive accuracy, the ANOVA remains a valid and powerful tool for identifying the relative significance and dominance of the influencing parameters.

The analysis of tool wear was divided into two metrics: wear length and flank wear width (V_B) as shown in Fig. 7. In these equations L1, L2, and β3 represent the wear length, wear width (V_B) and major cutting-edge angle. For wear length, the ANOVA, Table 6 revealed that the most dominant linear factor was depth of cut (p=0.001). A greater depth of cut increases the contact area and, consequently, the mechanical and thermal loads on the insert, accelerating wear progression along the cutting edge, as shown in Fig. 8.

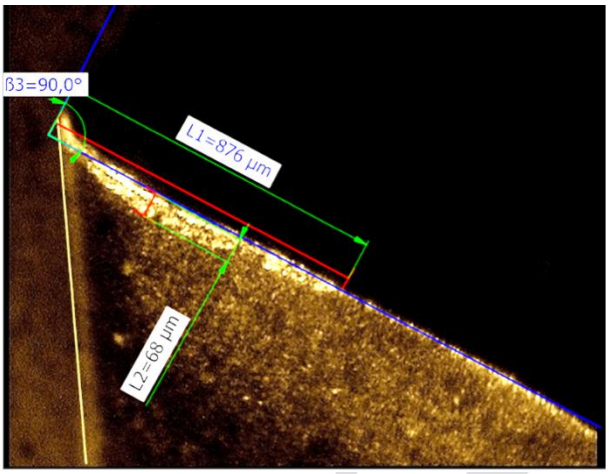

Fig. 7. Measurement result of tool wear width (V_B) and wear length on one of the inserts cutting tools.

Table 6. ANOVA of wear length.

Source	DF	Sum of Squares	Mean Squares	F	P-Value
Model	9	328826	36536	6.88	0.023
Linear	3	234561	78187	14.72	0.006
S	1	1343	1343	0.25	0.636
F	1	2358	2358	0.44	0.535
D	1	230860	230860	43.47	0.001
Square	3	88503	29501	5.55	0.048
S^2	1	61589	61589	11.60	0.019
F^2	1	1300	1300	0.24	0.642
D^2	1	28476	28476	5.36	0.068
2-WI	3	5762	1921	0.36	0.784
S*F	1	1820	1820	0.34	0.584
S*D	1	1508	1508	0.28	0,617
F*D	1	2434	2434	0.46	0.528
LoF	3	18390	6130	1.50	0.424
Pure Error	2	8166	4083	-	-
Total	14	355381	-	-	-

For flank wear width (V_B), the ANOVA revealed that the most significant influencing factor was the quadratic term of feed rate (p=0.004) as shown in Table 7. This indicates a strong non-linear relationship, suggesting that the wear progression does not increase or decrease monotonically but follows a more complex pattern. The physical mechanisms behind this can be explained by analysing the tool's behaviour at different feed rate regimes.

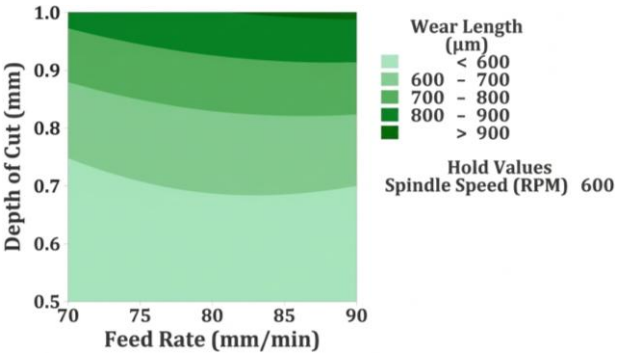

Fig. 8. Interaction between feed rate and depth of cut for wear length.

Table 7. ANOVA of V_B.

Source	DF	Sum of Squares	Mean Squares	F	P-Value
Model	9	475.998	52.889	4.35	0.060
Linear	3	62.472	20.824	1.71	0.280
S	1	10.125	10.125	0.83	0.404
F	1	2.347	2.347	0.19	0.679
D	1	50	50	4.11	0.099
Square	3	332.693	110.898	9.11	0.018
S^2	1	2.077	2.077	0.17	0.697
F^2	1	315.923	315.923	25.95	0.004
D^2	1	29.641	29.641	2.44	0.179
2-WI	3	80.833	26.944	2.21	0.205
S*F	1	13.444	13.444	1.10	0.341
S*D	1	0.694	0.694	0.06	0.821
F*D	1	66.694	66.694	5.48	0.066
LoF	3	49.306	16.435	2.84	0.271
Pure Error	2	11.556	5.778	-	-
Total	14	536.859	-	-	-

At very low feed rates, the undeformed chip thickness may become smaller than the cutting insert edge radius. Under such conditions, effective shearing is suppressed, and the cutting tool predominantly undergoes ploughing and rubbing against the workpiece surface. Instead of generating a continuous chip, the material experiences severe plastic deformation, followed by partial elastic recovery after tool passage [24]. This ploughing-dominated mechanism, coupled with prolonged tool–workpiece contact time and elevated frictional forces, facilitates the formation of a built-up edge (BUE). The inherent instability of the BUE promotes adhesive wear, wherein fragments intermittently detach from the adhered layer and damage the cutting edge [25]. As a result, attritious wear and micro-chipping develop on the rake face, which was experimentally observed at a spindle speed of 500 RPM and a feed rate of 70 mm/min, as shown in Fig. 9(a).

Interestingly, the maximum flank wear (V_B) was recorded at intermediate machining parameters, specifically at approximately 600 RPM and feed rates of 80–85 mm/min, as illustrated in Fig. 10. This behavior deviates from the conventional monotonic or simple U-shaped wear trends commonly associated with BUE stability, which typically suggest more pronounced wear at lower cutting speeds. A plausible explanation for this anomaly lies in the transitional nature of BUE behavior within the intermediate parameter regime. As reported by Ahmed et al. [25], BUE formed under such conditions is highly unstable and undergoes repeated cycles of formation and abrupt detachment. These violent detachment events induce severe abrasive action and repeated flaking on the tool surface, as evidenced by the wear morphology in Fig. 9(b).

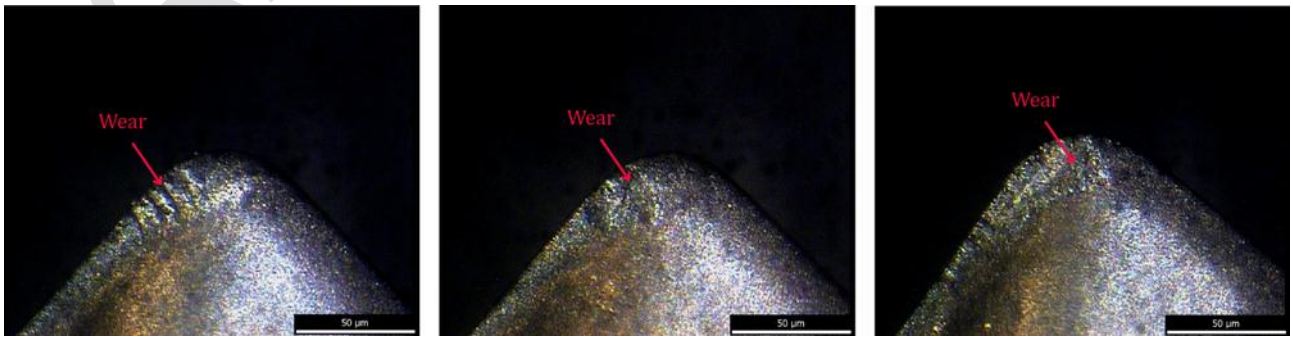

(a) (b) (c)

Fig. 9. Microscopic observation of tool wear types viewed from the rake face: (a) attritious wear and micro-chipping, (b) flaking, and (c) crater wear.

Consequently, accelerated flank wear and additional rake face degradation occur. This physical interpretation is strongly corroborated by the statistical analysis, wherein the significance of the quadratic term in the ANOVA confirms a pronounced non-linear relationship, with a distinct wear peak occurring at the mid-range parameter levels. At high feed rates, the increase in undeformed chip thickness leads to a substantial rise in cutting forces and thermal loads within the cutting zone [24]. The elevated temperatures soften the cutting tool material, thereby accelerating wear mechanisms dominated by thermal diffusion. In this process, tool material atoms diffuse into the hot, rapidly moving chip, resulting in pronounced crater wear on the rake face [26]. This wear mode was visually confirmed in the experiment conducted at a spindle speed of 700 RPM and a feed rate of 90 mm/min, as presented in Fig. 9(c).

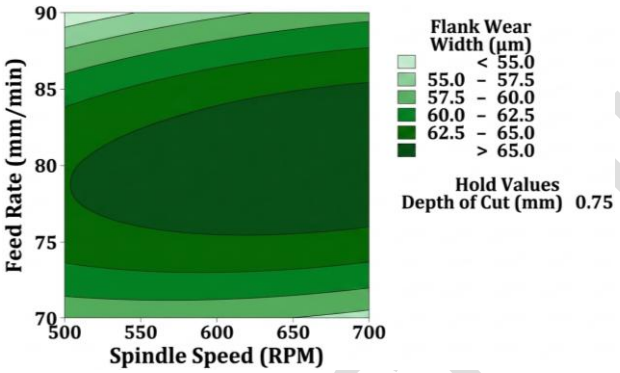

Fig. 10. Interaction between feed rate and spindle speed for flank wear width.

Given the competing influences of machining parameters on surface roughness, tool wear, and machining time, a multi-response optimization was performed using a desirability function approach to identify a single, balanced parameter set. The optimization objective for all three responses surface roughness, machining time, and tool wear was defined as "smaller is better." The desirability analysis, shown in Fig. 11, yielded an optimal combination of machining parameters comprising a spindle speed of 700 RPM, a feed rate of 70 mm/min, and a depth of cut of 1 mm. This parameter set represents an effective compromise that minimizes surface degradation and tool wear while maintaining acceptable productivity.

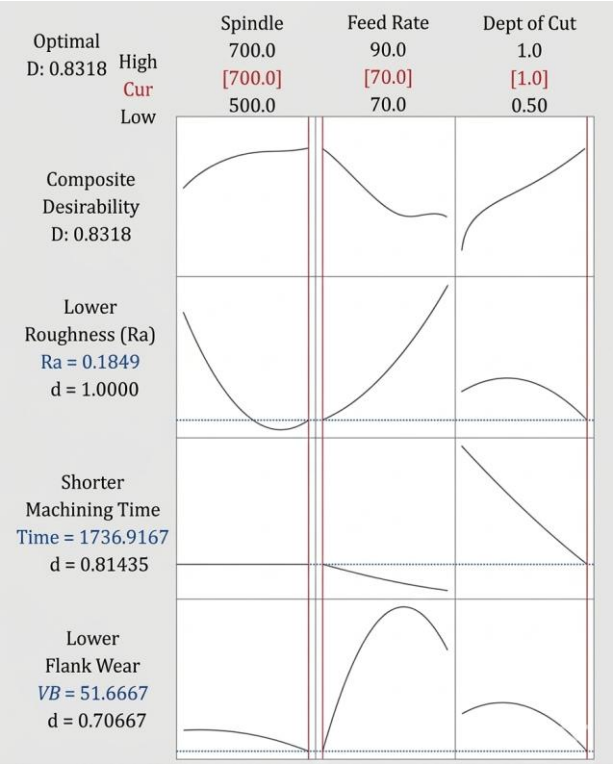

Fig. 11. Response optimization plot for surface roughness, machining time, and flank wear (V_B)

The optimal machining parameter combination is predicted to produce a surface roughness (Ra) of 0.185 µm, a machining time of 1737 s, and a flank wear width (V_B) of 51.67 µm. The resulting composite desirability value of 0.832 indicates a highly favourable compromise among the competing objectives. This high desirability score confirms that the identified parameter set effectively balances superior surface quality, acceptable machining productivity, and prolonged tool life, thereby demonstrating the robustness and practical relevance of the proposed multi-response optimization approach.

4. CONCLUSION

This study successfully investigated and optimized the CNC milling parameters for SUS316, focusing on the conflicting responses of surface roughness (R_a), machining time, and insert wear (V_B). Based on the experimental results and statistical analysis, the machining parameters exhibit different levels of influence on each response.

Surface roughness was most significantly affected by the linear effects of feed rate and spindle speed, as well as their interaction.

Machining time was predominantly controlled by depth of cut and feed rate. For tool wear, the depth of cut was the primary driver for wear length, while the quadratic effect of feed rate was the most significant factor for flank wear width (V_B), confirming a non-linear, U-shaped wear behaviour.

Due to the inherently conflicting nature of surface quality, productivity, and tool life in the milling of difficult-to-cut materials, a multi-response optimization based on a desirability function approach was implemented. The optimal machining parameter combination that achieves a balanced compromise among high surface quality (low Ra), improved productivity (short machining time), and enhanced tool longevity (low V_B) was identified as a spindle speed of 700 RPM, a feed rate of 70 mm/min, and a depth of cut of 1 mm.

The proposed optimal setting is predicted to yield a favorable performance combination, namely a surface roughness of 0.185 μm, a machining time of 1737 s, and a flank wear width (V_B) of 51.67 μm, corresponding to a high composite desirability value of 0.832. These results demonstrate the robustness and practical relevance of the adopted optimization framework and provide a validated parameter set for the reliable manufacturing of critical components from SUS316.

Future research is recommended to extend the present work by incorporating additional process variables, such as alternative cooling and lubrication strategies or advanced cutting tool geometries, to further improve machining efficiency and tool performance under industrial conditions.

Acknowledgement

The authors thank the Department of Mechanical Engineering, Vocational College of Universitas Gadjah Mada (DTM SV UGM) and PT Pupuk Bontang Indonesia for their laboratory and facility support during this research.

REFERENCES

[1] M. Sugavaneswaran, and A. Kulkarni, "Effect of Cryogenic Treatment on The Wear Behavior of Additive Manufactured 316L Stainless Steel", *Tribology in Industry*, vol. 41, No. 1, pp. 33-42, 2019, doi: 10.24874/ti.2019.41.01.04.

[2] Y. B. Lei, Z. B. Wang, B. Zhang, Z. P. Luo, J. Lu, and K. Lu, "Enhanced mechanical properties and corrosion resistance of 316L stainless steel by pre-forming a gradient nanostructured surface layer and annealing", *Acta Materialia*, vol. 208, pp. 116773, 2021, doi: 10.1016/j.actamat.2021.116773

[3] A. Equbal, M. A. Equbal, M. I. Equbal, P. Ravindrannair, Z. A. Khan, I. A. Badruddin, S. Kamangar, V. Tirth, S. Javed, and M. I. Kittur, "Evaluating CNC Milling Performance for Machining AISI 316 Stainless Steel with Carbide Cutting Tool Insert", *Materials*, vol. 15, no. 22, pp. 8051, 2022, doi: 10.3390/ma15228051.

[4] A. M. Philip and K. Chakraborty, "Some Studies on the Machining Behaviour of 316L Austenitic Stainless Steel", *Materials Today:Proceedings*, vol. 56, pp. 681–685, Jan, 2022, doi: 10.1016/j.matpr.2022.01.132.

[5] S. T. P. Kumar, H. P. Thirthaprasada, and M. Nagamadhu, "Multi-Response Optimization of Parameters in Turning of DSS-2205 using Hybrid (Al2O3+CuO) Nano Cutting Fluid with MQL", *Tribology in Industry*, vol. 42, no. 4, pp. 641-657, 2020, doi: 10.24874/ti.894.05.20.11.

[6] W. Ho, J. Tsai, and W. Huang, "Research on Surface Roughness of High-Speed Milling 7075-T6 Aluminum Alloy using Nanofluid/Ultrasonic Atomization Minimal Quantity Lubrication System", *Science Progress*, vol. 107, no. 4, pp. 1–21, 2024, doi.org/10.1177/00368504241284823.

[7] N. S. Kumar, A. Shetty, A. Shetty, K. Ananth, and H. Shetty, "Effect of Spindle Speed and Feed Rate on Surface Roughness of Carbon Steels in CNC Turning", *Procedia Engineering*, vol. 38, pp. 691-697, 2012, doi: 10.1016/j.proeng.2012.06.087.

[8] F. Ahmed, F. Ahmad, F. Abbassi, S. T. Kumaran, and T. Mabrouki, "Investigation of Machining Quality Indicators and Effect of Tool Geometry Parameters During the Machining of Difficult-To-Machine Metal", *Results in Materials*, vol. 20, pp. 100487, 2023, doi: 10.1016/j.rinma.2023.100487.

[9] J. A. Ghani, M. A. Ismanizan, H. A. Rahman, C. H. C. Haron, A. Z. Juri, M. S. Kasim, and M. Rizal, "Machining Analysis of S45C Carbon Steel Using Finite Element Method", *Jurnal Tribologi*, vol. 40, pp. 226-246, 2024,

[10] T. Mohanraj, S. Shankar, R. Rajasekar, N. R. Sakthivel, and A. Pramanik, "Tool Condition

Monitoring Techniques in Milling Process-A Review", *Journal of Materials Research and Technology*, vol. 9, iss.1, pp. 1032-1042, 2020, doi: 10.1016/j.jmrt.2019.10.031.

[11] M. Gdula, and G. Mrówka-Nowotnik, "Analysis of Tool Wear, Chip and Machined Surface Morphology in Multi-Axis Milling Process of Ni-Based Superalloy Using the Torus Milling Cutter", *Wear*, vol. 520–521, No. 15, May., pp. 204652, 2023, doi:10.1016/j.wear.2023.204652.

[12] R. G. Silva, R. L. Reuben, K. J. Baker, and S. J. Wilcox, "Tool Wear Monitoring of Turning Operations by Neural Network and Expert System Classification of a Feature Set Generated from Multiple Sensors", *Mechanical Systems and Signal Processing*, vol. 12, no. 2, pp. 319–332, 1998, doi: https://doi.org/10.1006/mssp.1997.0123.

[13] ISO 8688-2:1988, Tool Life Testing in Milling-Part 2: End Milling, 1988.

[14] H. Hassanpour, A. Rasti, J. H. Khosrowshahi, and S.S. Farshi, "Effect of Ball Nose Flank Wear on Surface Integrity in High-Speed Hard Milling of AISI 4340 Steel Using MQL", *Heliyon*, vol. 10, Iss. 18, pp. e37337, 2024, doi: 10.1016/j.heliyon.2024.e37337.

[15] M. Shah, V. Vakharia, R. Chaudhari, J. Vora, D. Y. Pimenov, and K. Giasin, "Tool Wear Prediction in Face Milling of Stainless Steel using Singular Generative Adversarial Network and LSTM Deep Learning models", *International Journal of Advanced Manufacturing Technology*, vol. 121, no. 1–2, pp. 723–736, Jul. 2022, doi: 10.1007/s00170-022-09356-0.

[16] A. B. Shelar, P. G. Student, and A. M. Shaikh, "Optimization of Process Parameters in Milling of Stainless Steel 316 Using Coated Insert and MEGA Coated Inserts", *International Journal of Emerging Technologies in Engineering Research (IJETER)*, vol. 6, no. 9, pp. 25–33, 2018.

[17] D. Shinde and V. S. Jadhav, "Optimizing Machining Parameters for End Milling 316l Stainless Steel under Dry Conditions", *International Journal of Engineering Research in Mechanical and Civil Engineering*, vol.11, iss. 8, pp.25-33, 2024.

[18] I. P. Okokpujie, L. K. Tartibu, and K. Okokpujie, "Implementation of Box–Behnken design to study the factors interaction impacts and modelling of the surface roughness of AL 6063 alloys during turning operations", *International Journal on Interactive Design and Manufacturing (IJIDeM)*, vol. 18, pp. 6531–6541, 2024, doi: 10.1007/s12008-023-01278-9.

[19] M. Manohar, J. Joseph, T. Selvaraj, and D. Sivakumar, "Application of Box Behnken Design to Optimize the Parameters for Turning Inconel 718 Using Coated Carbide Tools", *International Journal of Scientific & Engineering Research*, vol. 4, iss. 4, pp.620-642, 2013.

[20] L. W. Hernández-González, R. Pérez-Rodríguez, A.M. Quesada-Estrada, and L. Dumitrescu, "Effects of Cutting Parameters on Surface Roughness and Hardness in Milling of AISI 304 Steel", *DYNA*, vol. 85, no. 205, pp. 57-63, 2018, vol. 85, no.205, pp. 57–63,201 8, doi: 10.15446/dyna.v85n205.64798.

[21] L. Peña-Parás D. Maldonado-Cortés, M. Rodríguez-Villalobos, A. G, Romero-Cantú, O. E. Montemayor, M. Herrera, G. Trousselle, J. González, and W. Hugler, "Optimization of Milling Parameters of 1018 Steel and Nanoparticle Additive Concentration in Cutting Fluids for Enhancing Multi-Response Characteristics", *Wear*, vol. 426–427, pp. 877–886, 2019, doi: 10.1016/j.wear.2019.01.078.

[22] L. Peña-Parás, M. Rodríguez-Villalobos, D. Maldonado-Cortés, J. A. González-García, M. Herrera-Maldonado, G. Trousselle-Strozzi, O. E. Montemayor, A. G, Romero-Cantú, and D. I. Quintanilla-Correa, "Optimizing Milling Parameters and Halloysite Nanotube Concentration to Enhance Surface Quality and Reduce Energy Consumption", *Tribology in Industry*, vol. 47, no. 2, pp. 313–325, 2025, doi: 10.24874/ti.1896.02.25.04.

[23] M. R. Policena, C. Devitte, G. Fronza, R. F. Garcia, and A. J. Souza, "Surface Roughness Analysis in Finishing End-Milling of Duplex Stainless Steel UNS S32205", *International Journal of Advanced Manufacturing Technology*, vol. 98, no. 5–8, pp. 1617–1625, 2018, doi: 10.1007/s00170-018-2356-4.

[24] G. Sur, A. R. Motorcu, and S. Nohutçu, "Single and Multi-Objective Optimization for Cutting Force and Surface Roughness in Peripheral Milling of Ti6Al4V using Fixed and Variable Helix Angle Tools," *Journal of Manufacturing Processes*, vol. 80, pp. 529–545, 2022, doi: 10.1016/j.jmapro.2022.06.016.

[25] S. Y. Ahmed, J. M. Paiva, B. Bose, and S. C. Veldhuis, "New Observations on Built-Up Edge Structures for Improving Machining Performance during the Cutting of Superduplex Stainless Steel," *Tribology International*, vol. 137, pp. 212–227, 2019, doi: 10.1016/j.triboint.2019.04.039.

[26] A. H. Musfirah, J. A. Ghani, and C. H. Che Haron, "Tool Wear and Surface Integrity of Inconel 718 in Dry and Cryogenic Coolant at High Cutting Speed," *Wear*, vol. 376–377, pp. 125–133, 2017, doi: 10.1016/j.wear.2017.01.031.